THE JOURNAL OF PHYSICAL CHEMISTRY C
A JOURNAL OF THE AMERICAN CHEMICAL SOCIETY

pubs.acs.org/JPCC

Review

Electrolyte Effect on Electrochemical CO_2 Reduction to Multicarbon Products

Published as part of The Journal of Physical Chemistry C virtual special issue "Jens K. Nørskov Festschrift".

Xian Zhong, Hong-Jie Peng, Chuan Xia,* and Xinyan Liu*

Cite This: https://doi.org/10.1021/acs.jpcc.4c00021

Read Online

ACCESS | Metrics & More | Article Recommendations

ABSTRACT: The ever-growing environmental concern has yielded the electrocatalytic carbon dioxide reduction (eCO_2R) center of research attention, as it offers a possible pathway to achieve net-zero carbon emission and realize a post-fossil-fuel society. The production of multicarbon (C_{2+}) species with higher energy density is more desirable but unfortunately presents a greater challenge. Other than the catalyst itself, the electrolyte has also been demonstrated to exhibit nontrivial impacts on eCO_2R, a systematic understanding on the effect of which therefore remains vital. In this Review, we thoroughly discussed the influence that electrolytes might induce on eCO_2R from three perspectives, namely, pH, cations, and anions. Both experimental and theoretical efforts are included, along with the hypothesis on the fundamental working mechanism. We also highlighted the challenges associated with understanding and harnessing the electrolyte effect, as well as theoretical modeling and machine learning as interesting directions worthy of further research and exploration. We believe that this Review can help to shed light on the rational design and optimization of electrolytes, thereby facilitating the activity tuning and selectivity steering of eCO_2R to valuable C_{2+} products.

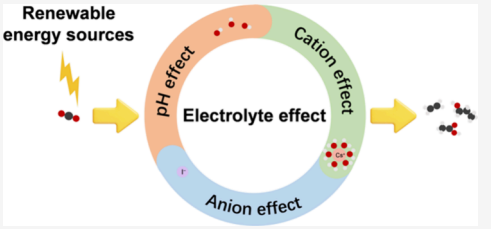

1. INTRODUCTION

Electrochemical carbon dioxide reduction (eCO_2R) has received lots of research and industrial attention due to its mild reaction conditions (e.g., room temperature and atmospheric pressure) and the ability to produce valuable fuels and chemicals leveraging electricity derived from intermittent renewable sources (such as wind, solar, and tidal energy).[1−4] With the huge potential to facilitate the replacement of coal-fired power generation with clean energy generation, this technology remains vital in reducing industrial carbon emissions. Up to now, remarkable progress has been made in the production of C_1 products (e.g., carbon monoxide (CO),[5−8] formic acid (HCOOH),[9−13] methane (CH_4),[14−16] methanol (CH_3OH)[17−19]) from eCO_2R, where decent activity and Faradaic efficiency (FE) can be achieved as these reactions generally involve fewer proton and electron transfers. The generation of multicarbon (C_{2+}) products that deliver higher energy densities,[20−22] however, presents greater economic attraction and unfortunately also a larger challenge. The involvement of more elementary steps and side reactions has complicated the activity optimization and selectivity tuning toward a specific product, yielding the study on this reaction also of great scientific significance, as tailoring product selectivity remains a key challenge in heterogeneous catalysis.

At present, a large number of experimental and theoretical studies for eCO_2R to C_{2+} products have been focused on the development of catalysts (Cu-based and non-Cu-based catalysts). In order to enhance the electrocatalytic performance, various efforts have been devoted to designing low-coordination sites and defects,[23] altering the size and shape of the nanostructures,[25] tuning the oxidation state,[26,27] and adding auxiliary metals.[24] Apart from optimizing the catalyst itself, tuning the electrolyte has alternatively been demonstrated essential in improving C_{2+} production, as the influence of the reaction microenvironment remains nontrivial. For instance, it was recently found from experiments and computational modeling that the activity of C_{2+} product formation in eCO_2R is dependent on both the pH and the identity of ions present in the electrolyte solutions. By rationally designing the pH and ions in the electrolyte, the overpotential of C_{2+} products can potentially be drastically reduced, improving the energetic efficiency of eCO_2R to C_{2+} products.[28−30] However, the effect of electrolytes on reaction activity and selectivity can be convoluted and is often dependent on many factors such as the reaction condition or the catalytic system investigated. In addition, consensus is still

Received: January 2, 2024
Revised: February 8, 2024
Accepted: February 8, 2024

lacking regarding the internal mechanism of the electrolyte effect. It is therefore necessary to systematically understand the effects that electrolytes might induce on eCO_2R as well as the corresponding working principles.

In this work, we present a comprehensive discussion focusing on the electrolyte effect regarding the production of C_{2+} species from eCO_2R. The experimental and theoretical evidence on the significance of C−C bond formation for C_{2+} production is first reviewed using CO dimerization as an example, which yields *OCCO dimer as the initial backbone of C_{2+} products. We then discuss how *OCCO formation and other key elementary steps might be impacted by the electrolyte from three perspectives, namely, pH, cations, and anions (Figure 1). Lastly, possible future directions to enhance eCO_2R to C_{2+} products are envisioned and key challenges to improve C_{2+} selectivity are identified.

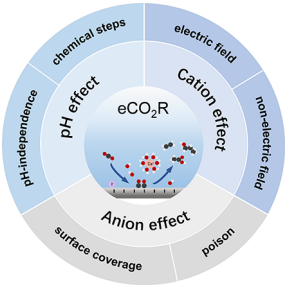

Figure 1. Electrolyte effect for eCO_2R to C_{2+} products.

2. C−C BOND FORMATION

C−C bond formation is deemed the most crucial step in C_{2+} production, which is likely to occur by the coupling of two CO molecules as proposed by Schouten et al.[31] Using operando Raman spectroscopy combined with density functional theory (DFT), Zhan et al. unraveled the potential dependence of the Raman peak ratio of Cu−CO stretching and the restricted rotation of adsorbed *CO. Such a ratio was further shown to correlate with *CO coverage on the electrode surface, the preferred binding sites of *CO, and the selectivity of C_{2+} product.[32] Specifically, the higher Raman peak ratio at more negative potential (or with higher CO concentration) corresponded to a higher *CO coverage, as well as a larger population of weakly bound *CO at the atop site. The DFT calculations showed that when at least one *CO atop was involved in the formation of *OCCO, the CO−CO coupling exhibited substantial decrease in coupling barriers. Similarly, leveraging the time-resolved surface-enhanced Raman spectroscopy technique, An et al. found a highly dynamic *CO intermediate, with a characteristic Raman peak below 2060 cm^{-1}, to predominantly associate with *OCCO formation while the *CO intermediate with a characteristic Raman peak at 2092 cm^{-1} was identified as the source of desorbed *CO product.[33] These works highlight the crucial role of specific *CO binding configurations to trigger *OCCO formation, as well as the highly dynamic nature of CO−Cu interactions under different potentials. In addition, the existence of *OCCO can be substantiated by the presence of its reduction product *OCCOH, which was experimentally detected via vibrational analysis using Fourier transform infrared spectroscopy (FTIR) spectroscopy.[34]

Apart from experimental measurements, a great deal of theoretical effort has also been devoted to highlighting the significance of *OCCO. For instance, Calle-Vallejo et al. utilized DFT calculations to propose that the formation of *OCCO by coupling *CO with gas-phase CO via electron transfer (ET) at Cu(100) is the rate-limiting step (RLS).[35] Meanwhile, *OCCO was found to have good electron affinity and remain susceptible to electron−proton decoupling, explaining the high selectivity of electrochemical carbon monoxide reduction (eCOR) toward ethylene (C_2H_4) at low overpotentials. Alternatively, Montoya et al. adopted explicit water layers to simulate electrochemical conditions on Cu(111) and Cu(100) with the effect of solvents taken into account. They demonstrated that the combined effect of solvation and localized electric fields can thermodynamically and kinetically reduce the energy required for the generation of *OCCO from *CO, yielding the coupling of *CO the preferred pathway instead.[36] Similarly, Hedström et al. demonstrated a significant stabilizing effect of solvation on highly polar *OCCO using the implicit solvent model and the hybrid solvent model,[37] accentuating the key role of *OCCO in eCO_2R. Of course, many other C−C coupling intermediates have also been found important and discussed elsewhere,[38−40] such as $*OCCH_x$,[41,42] *OCCHO,[43−47] *CCO,[22] $*CH_2CH_2$,[48] $*COCH_3$,[49] etc. For simplicity, we will primarily focus on the electrolyte effect on *OCCO in this Review, while many other intermediates can be derived from it and exhibit similar response to variations in the electrolyte.

3. ELECTROLYTE EFFECT

The choice of electrolyte can introduce a number of intriguing impacts on the local reaction environment and thereby affect the final activity and selectivity of eCO_2R. For instance, the composition and concentration of anions and cations can induce variations in the local pH,[50] electrostatic interactions,[51] buffer capacity,[52] and surface coverage.[53] The entangled nature of these factors often further complicates electrolyte optimization and rational design, as it is hardly possible to isolate a single effect. In this section, we will discuss how various electrolyte-related properties (pH) and species (cations, anions) can impact eCO_2R.

3.1. pH Effect. pH describes the proton concentration in a solution. Since many cathodic half-reactions in eCO_2R involve the transfer of proton−electron pairs, the availability of protons presents one of the major factors influencing the reaction activity and selectivity. Experimentally comparing the onset potentials vs standard hydrogen electrode (SHE) of C_{2+} products in eCO_2R and eCOR at pH = 7 and pH = 13 on Cu, Wang et al. have interestingly discovered that C_{2+} formation did not vary with pH and described this invariance as pH independence.[28] This coincides with the early experimental observation by Hori et al., who found that the RLS to C_{2+} products such as C_2H_4 showed good linear correlations with potential and was independent of pH on the SHE scale by comparing the partial currents of different products (CH_4, C_2H_4, and C_2H_5OH) as a function of the electrode potential.[54,55] Previously, this pH independence of C_{2+} formation was thought to be related to the decoupling of protons from electrons in the RLS, as well as the slower rate of ET compared to proton transfer (PT).[35,43] However, the very broad energy distribution of adsorbates on the metal surface leads to a smaller energy level difference in ET, implying a rather facile ET which is unlikely to be the RLS in eCO_2R.[56]

https://doi.org/10.1021/acs.jpcc.4c00021
J. Phys. Chem. C XXXX, XXX, XXX−XXX

Alternatively, the pH independence can be rationalized by the proton source. As revealed by Wang et al., who took the Volmer reaction as an example, the activation energy is only affected by the SHE potential when the proton involved originates from water (Figure 2a).[28] In the case of eCO_2R, Liu

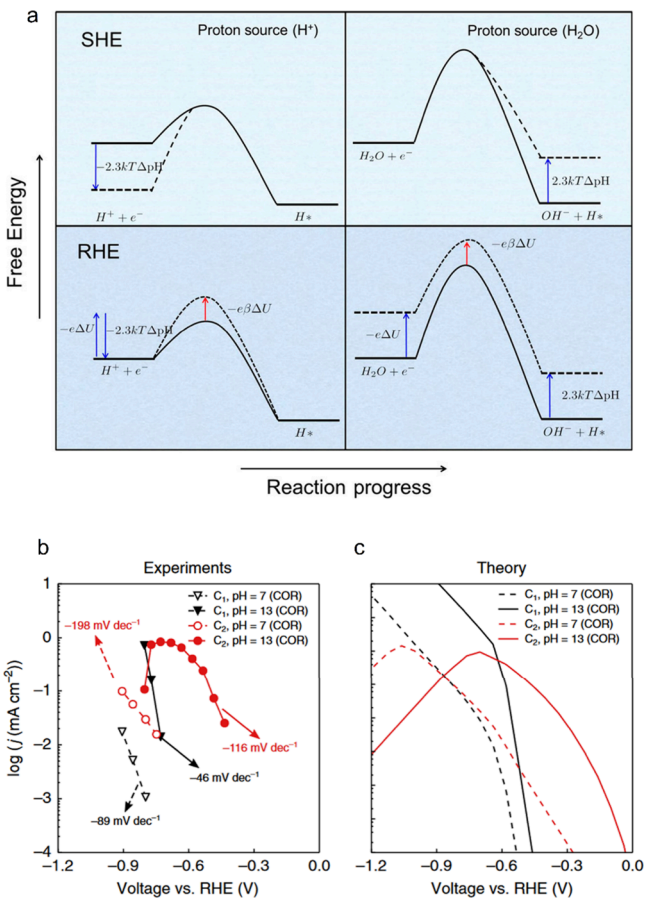

Figure 2. pH independence of C_{2+} products. (a) Activation energies for Volmer reaction on the SHE and RHE scales, where protons in PCET originate from H^+ (acidic) or water (alkaline), respectively. Reproduced from ref 28 with permission. Copyright 2018 American Chemical Society. (b) Experimentally measured polarization curves for eCOR on polycrystalline Cu at pH = 7 and pH = 13. (c) Predicted polarization curves from the microkinetic model for eCOR at pH = 7 and pH = 13. Reproduced from ref 57 with permission. Copyright 2019 The Authors.

et al. further elaborated the pH effect on steering the product selectivity.[57] For a RLS involving proton-coupled electron transfer (PCET) from water to adsorbate X under alkaline or neutral conditions, the reaction rate based on the Butler–Volmer equation can be expressed as

$$R = A\theta_{*X}\exp\left(-\frac{G_a^0 + e\beta U_{SHE}}{kT}\right) \quad (1)$$

where A is the prefactor, θ_{*X} is the coverage of *X, G_a^0 is the activation energy at U_{SHE} = 0 V, β is the transfer coefficient (i.e., the amount of charge transferred to the transition state), U_{SHE} is the potential vs SHE, k is the Boltzmann constant, and T is the reaction temperature. Under the assumption that the elementary reaction steps prior to the RLS (m*CO + n(H_2O + e^-) ↔ *X + $n$$OH^-$) are in quasi-equilibrium, θ_{*X} could then be expressed in terms of θ_{*CO} as

$$\theta_{*X} = \theta_{*CO}^m \exp\left(-\frac{\Delta G^0 + enU_{RHE}}{kT}\right) \quad (2)$$

where m is the number of *CO involved in reactions before the RLS, ΔG^0 is the free energy of X* formation from CO at 0 V vs reversible hydrogen electrode (RHE), U_{RHE} is the potential vs RHE, and n is the number of PCET steps before RLS. Since U_{RHE} and U_{SHE} are interchangeable using the Nernst equation ($U_{RHE} = U_{SHE} + \frac{2.3npH}{kT}$), θ_{*X} will be pH-dependent on the SHE scale if $n > 0$. Combining all above expressions, the overall rate can be written as

$$R = A\theta_{*CO}^m \exp\left(-\frac{G_a^0 + \Delta G^0}{kT} - \frac{\beta + n}{kT}eU_{SHE} - 2.3npH\right) \quad (3)$$

When the C_2 formation is limited by the protonation of *OCCO, namely, the first PCET (n = 0), the overall reaction rate becomes dependent only on U_{SHE}. And the C_{2+} products will exhibit pH independence on the SHE scale. On the other hand, the competing pathway to form C_1 species exhibits a different pH dependence because of the late RLS (i.e., $n > 0$) for C_1 formation.[57] A pH-dependent microkinetic model using energetics estimated via explicit solvent simulations was then established, which showed qualitative and even semiquantitative agreement with experimental observations (Figure 2b,c). C_2 production at low overpotentials was shown to be limited by the first PCET further confirming the hypothesis of an *OCCO mechanism, while a later PCET to form *CH in the sequential reduction of CO (*CO → *CHO → *CHOH → *CH) was found to limit C_1 formation, resulting in a much smaller enhancement in C_1 activity when increasing pH at the RHE scale. Consequently, high alkaline conditions can effectively increase the selectivity of eCO_2R and eCOR to C−C coupling products. Further expanding this kinetic model to the understanding of product selectivity among C_2 hydrocarbons and oxygenates, Peng et al. also suggested that the difference in RLSs for C_2 hydrocarbon and oxygenate formation bifurcating from a common dehydrogenated ketene intermediate (*CHCO), as well as the potential dependence of these RLSs, could rationalize the trend in C_2 hydrocarbon/oxygenate selectivity over a broad range of Cu-based catalysts.[21] Through explicit reaction thermodynamics and kinetics calculation, they found the RLS for C_2 oxygenate formation to be *CHCO → CH_2CO or *OCHCH (n = 0, relative to *CHCO) while the RLS for C_2 hydrocarbon formation to be *CHCOH → *CCH (n = 1) at low overpotential and *CHCO → *CHCOH (n = 0) at high overpotential. The fact that the C_2 hydrocarbon pathway suffers from an additional energetic penalty from the dehydroxylation step of CHCOH* under alkaline condition presents the main reason for the exceptionally high selectivity of any C_2 oxygenate species (not just acetate as we discussed later) at low overpotential. Based on the prerequisite that water serves as the proton donor, these works present a general understanding of the pH effect in neutral and alkaline electrocatalysis.

In addition, different pH levels can also open up distinct reaction pathways of eCOR toward C_1 and C_{2+} products. For instance, Xiao et al. adopted an implicit solvation model to describe the realistic electrochemical interface on Cu(111) and to obtain accurate starting electrochemical potentials.[58] By

https://doi.org/10.1021/acs.jpcc.4c00021
J. Phys. Chem. C XXXX, XXX, XXX−XXX

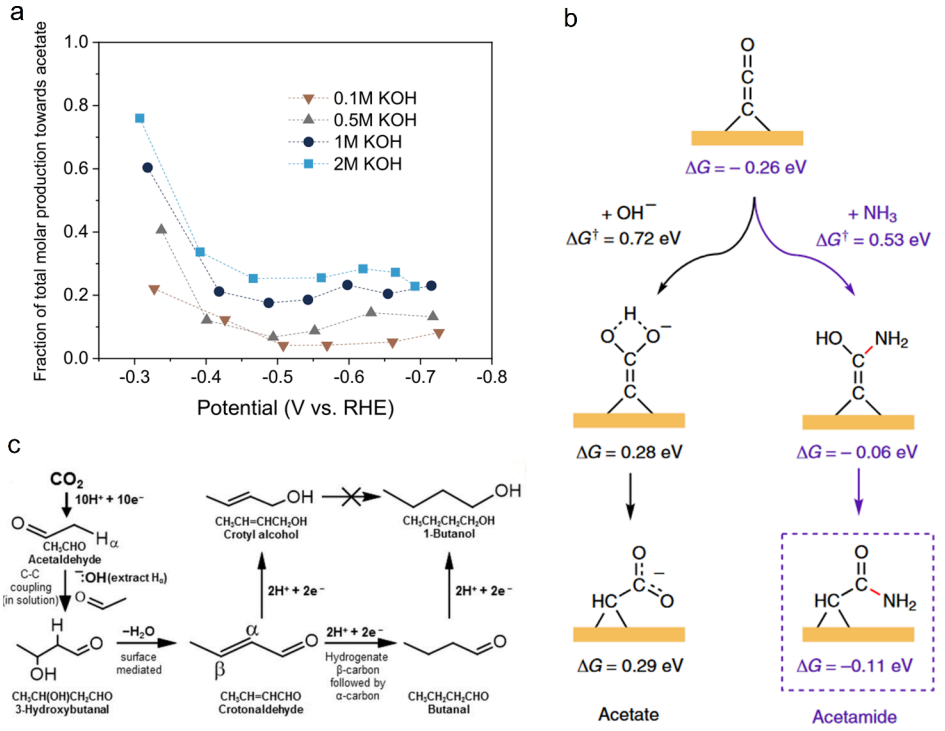

Figure 3. Catalytic effect on chemical reactions in eCO_2R. (a) Ratio of molar yield of acetate to total molar yield of eCOR on "oxide-derived" copper at various KOH concentrations from 0.1 to 2.0 M. Reproduced from ref 60 with permission. Copyright 2018 The Authors. (b) Reaction mechanism for the reduction of *CCO intermediate to acetate at high pH. Reproduced from ref 61 with permission. Copyright 2019 The Authors. (c) Reaction mechanism of eCO_2R to 1-butanol. For simplicity, the reaction steps involving multistep PCET are replaced by $nH^+ + ne^-$. Reproduced from ref 63 with permission. Copyright 2020 The Authors.

comparing the kinetic activation energies, it was found that the C_1 pathway generates CH_4 via *COH to *CHOH under acidic conditions at pH = 1, while the C_{2+} pathway is kinetically blocked. Under neutral conditions at pH = 7, the C_{2+} production is realized by the CO−COH coupling with a common intermediate *COH sharing with the C_1 pathway. At high pH = 12, early C−C coupling forming adsorbed *OCCO dominates, thereby kinetically inhibiting the C_1 production and increasing the selectivity of C_{2+} species.

Other than PCET, the chemical reaction catalyzed by hydroxide (OH^-) also plays an important role in the generation of C_{2+} products. Online electrochemical mass spectrometry (OLEMS) was utilized by Birdja et al. to demonstrate that OH^- promoted C_2 and C_3 aldehydes with a Cannizzaro-type disproportionation, which led to the formation of corresponding carboxylic acid and alcohol.[59] Jouny et al. found that the selectivity of acetic acid improved with increasing electrolyte pH by varying the concentration of KOH in the range 0.1−2.0 M (Figure 3a).[60] Using labeled $C^{18}O$ gas, they found that OH^- can attack the ketene-like intermediate to promote acetate production under highly alkaline conditions. Full-solvent quantum mechanical calculations were also performed to validate the viability of OH^- reacting with *CCO to produce acetate from a theoretical point of view, where the energetic barrier was indeed found surmountable (Figure 3b).[61] Interestingly, Heenen et al. utilized ab initio simulation to establish a coupled kinetic-transport model on Cu and proposed a new reaction mechanism for acetate formation, which was used to explain the experimental observation that acetate selectivity increases with pH.[62] They suggested that *CHCO is simultaneously reduced and further desorbed to ketene (CH_2CO) in solution, and this stable close-shell molecule reacts with OH^- to form acetate anion (CH_3COO^-). At the same time, both CH_3COO^- and the electrode surface are negatively charged. The electrostatic repulsion thereby leads to a preference for $CHCOO^-$ diffusing into the electrolyte rather than readsorption and further reduction to other C_2 products. The presence of OH^- in the electrolyte can also have a non-negligible effect on the generation of additional reduced products, such as C_4 species. For instance, Ting et al. reported that the high local pH could promote acetaldehyde production, which is reduced to butanal and finally 1-butanol through a base-catalyzed aldol condensation to crotonaldehyde (Figure 3c).[63] Therefore, high pH not only improves the selectivity of C_{2+}/C_1 but also modulates the distribution within the C_{2+} products, where the influence brought by local concentration of pertinent species remains nontrivial.

While research evidence has suggested that increasing the pH is an effective way to increase C_{2+} activity and selectivity, we also note that the reaction between CO_2 and OH^- is an additional modulator of local pH, which is greatly affected by the mass transport of CO_2 and OH^-. Raciti and Lum et al. have adopted a numerical model to reveal such a relationship by plotting the C_{2+} selectivity map with local pH as a descriptor on various oxide-derived catalysts.[64,65] They found that the hydrogen evolution reaction (HER) became dominant at higher pH due to the mass transport limitation of CO_2 and the optimal local pH range laid around 9−10. In brief, the high pH conditions and sufficient mass transport of CO_2 remain essential in promoting eCO_2R to C_{2+} products. For practical CO_2 electrolysis, gas diffusion electrode (GDE)-based flow cells have been developed to overcome the above CO_2 transport limitation and improve the maximum achievable

https://doi.org/10.1021/acs.jpcc.4c00021
J. Phys. Chem. C XXXX, XXX, XXX−XXX

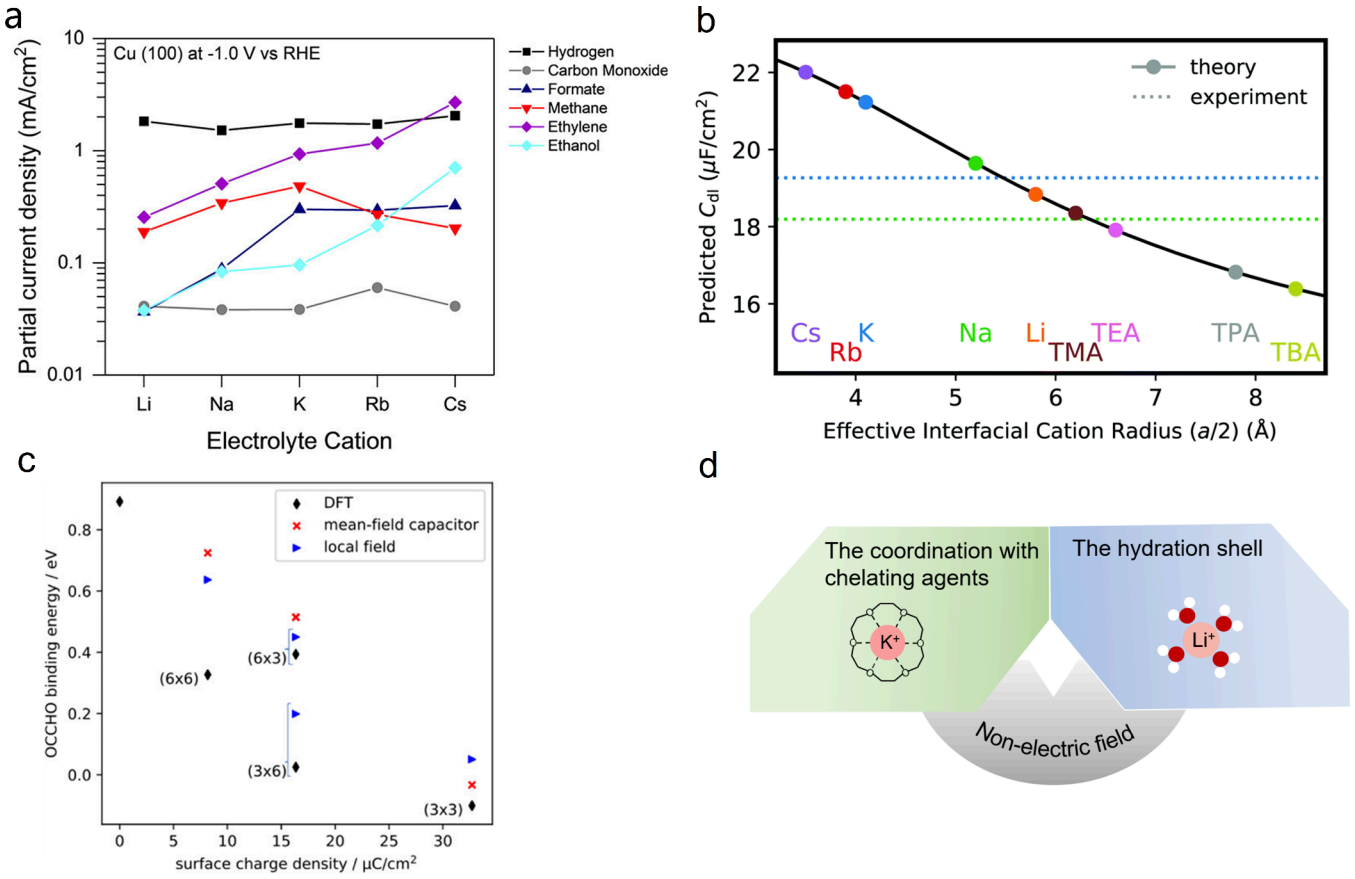

Figure 4. Cation effect for eCO_2R to C_{2+} products. (a) Effect of different cations on the partial current density of the major product of eCO_2R on Cu(100) at −1.0 V vs RHE. Reproduced from ref 30 with permission. Copyright 2017 American Chemical Society. (b) Cation size as a function of double layer capacitance on Au(111) single crystal electrode. Reproduced from ref 51 with permission. Copyright 2019 RSC Publishing. (c) Dependence of *OCCHO binding energy on explicit surface charge density under DFT, capacitor and local field models. Reproduced from ref 73 with permission. Copyright 2020 American Chemical Society. (d) Nonelectric field effect of cations on eCO_2R.

current density. Due to the drastic increase in operating current density and the consumption of water as a proton source, the local pH increases dramatically near the electrolyte/cathode interface even in an electrolyte with near-neutral bulk pH. An excessively high local pH thus also increases the susceptibility of CO_2 to OH^- attack to generate more bicarbonate and carbonate, which in contrast induces a decrease in eCO_2R selectivity and overall carbon efficiency. Therefore, the mass transport limitation of CO_2 and high local pH inextricably intertwine, resulting in complex influence on the final eCO_2R activity and selectivity. For the sake of decoupling such a tangled influence, tandem reactor design could be a promising direction by sequencing an alkaline electrolyzer for eCOR to C_{2+} products after an acidic or solid-oxide electrolyzer for eCO_2R to CO.[66] Such a flexible design allows for targeted optimization of each electrolyzer and circumvents the issue of side reaction between CO_2 and OH^- that leads to detrimental carbonate formation and a decrease in local pH.

3.2. Cation Effect. In the electrolyte, the supporting salt is adopted to increase the solution ionic conductivity, which also introduces anions and cations. From this section we begin to elaborate on the effect brought by these ions, starting with the cations. The most common cations in eCO_2R are alkali metal cations, which can affect the kinetic potential required for C_{2+} production by inducing variations in local pH.[50] In bicarbonate solutions, the hydration radius of cation increases as the cation radius decreases, leading to improved cation adsorption. Such enhancement can result in positive Outer Helmholtz Plane (OHP) potential and promote HER, which in return impacts the local pH and increases C_2 selectivity.[67,68] On the other hand, a larger cation radius strengthens the Coulombic interaction between the cation and the negative charge on the cathode, causing the hydrolysis equilibrium constant (pK_a) of the cation to decrease and making it more susceptible to hydrolysis to release protons. In this case, the buffered local pH can also increase the concentration of CO_2, and thereby promote the eCO_2R activity.[69]

In addition to local pH, cations have also been found to influence the reaction through other factors, such as the electrostatic field. As shown in Figure 4a, Resasco et al. discovered that the rates of C_2H_4 and C_2H_5OH formation increased monotonically with cation size by applying a sufficiently low voltage (U_{RHE} = −1 V) in Cu(100).[30] In conjunction with DFT calculations, they rationalized this large influence through the decreased reaction energies of elementary steps involving species with strong dipole moments caused by the cation-induced local electrostatic field. As typical C_2 intermediates such as *OCCO exhibit greater polarities than C_1 intermediates, they are more stabilized comparing to C_1 intermediates under the same electric field strength. The cations therefore can enhance the selectivity of C_2 products via induced electrostatic field. The strength of such field is further found to be dependent on the cation coverage at the

https://doi.org/10.1021/acs.jpcc.4c00021
J. Phys. Chem. C XXXX, XXX, XXX−XXX

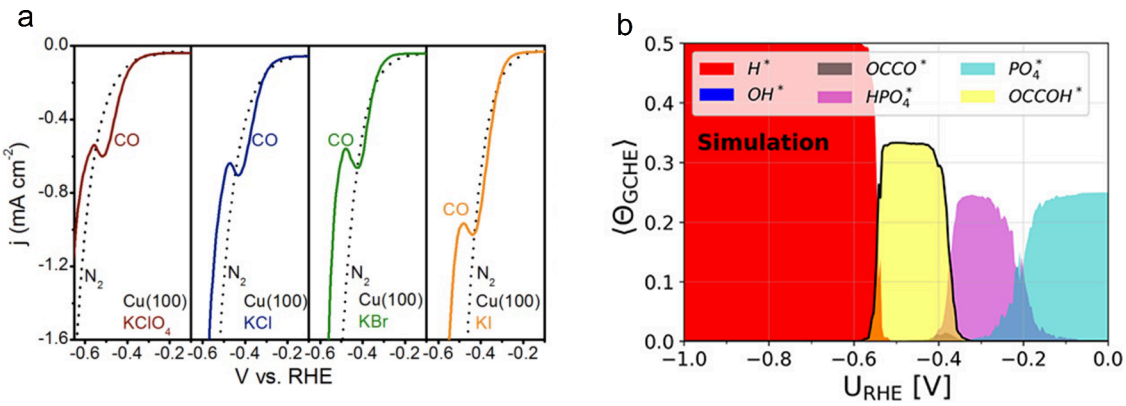

Figure 5. Anion effect for eCO_2R to C_{2+} products. (a) Linear sweep voltammograms of Cu(100) electrodes in electrolytes containing different anions. Reproduced from ref 53 with permission. Copyright 2018 John Wiley and Sons. (b) Coverage $\langle\Theta_{GCHE}\rangle$ of each relevant species on Cu(100) as a function of U_{RHE} at pH = 7 with phosphate ion electrolyte. Reproduced from ref 79 with permission. Copyright 2019 American Chemical Society.

Helmholtz plane. For instance, Ringe et al. have proposed a multiscale modeling approach to quantitatively characterize the effect of cation size on interfacial electric field.[51] The cations in the Helmholtz layer were revealed to affect the cation concentration and double layer capacitance through mutual repulsion with water. As shown in Figure 4b, the double layer capacitance of the Au(111) electrode increased with decreasing hydrated cations radius at the same potential of zero charge (PZC), resulting in enhanced surface charge density and consequently stronger interfacial electric field. Similarly, Gunathunge et al. experimentally demonstrated that the concentration of cation in the outer Helmholtz layer increased with its size, and a stronger interfacial electric field can be observed with attenuated total internal reflection Fourier transform infrared spectroscopy (ATR-FTIR), leading to a subsequent promotion in COR kinetics.[70] At the same time, the cation promoter effect was also revealed to be potential- and structure-dependent, as discovered by Pérez-Gallent et al. using FTIR and DFT calculations.[71] At low overpotentials, larger cations steered eCO_2R selectivity toward C_{2+} products, where the onset potential showed great sensitivity to cation size and electrode structure. However, at high overpotentials the onset potential for methane remained rather independent of the cation radius and electrode structure. Along the same line, Ren et al. also investigated the variations in optimal electrolyte concentration when potential changes,[72] and it was demonstrated that lower cation concentrations were required to balance the surface charge density to achieve the same optimal field strength at a higher applied potential. In addition to concentration and applied potential, the interfacial electric field is also influenced by the spatial distribution of the cations, as shown by Ludwig et al. with minima hopping calculations. They revealed that the localized electrostatic field was sensitive to the geometrical distribution of the surface charge at a given charge density.[73] With *OCCHO as an example, they showed that its binding energy depended strongly on the spatial distribution of cations at the same surface charge density (Figure 4c), emphasizing on the necessity of considering the local electrostatic field generated by cations for C_{2+} production.

Besides the electrostatic effect, alkali metal cations can also impact the production of C_{2+} chemicals through nonelectric field interactions (Figure 4d). For instance, using spectroscopic studies, Malkani et al.[74] found that the eCOR rate varied with K^+, Rb^+, and Cs^+, despite the fact that they all possessed nearly identical interfacial electric field strengths as represented by Stark tuning rates, suggesting the existence of the nonelectric field effect. They further hypothesized that such an effect may be related to the structure of alkali metal cation and interfacial water interactions, such as the looseness or tightness of the hydration shell and the coordination with chelating agents such as crown ethers, which affected the chemistry of alkali metal cations with the reaction intermediates and consequently the rate of reaction. Interestingly, Liu et al. proposed another "cation intermediate complex" mechanism to rationalize alkali metal cation promotion at the atomic/molecular level.[75] Using ab initio molecular dynamics (AIMD) simulation and free-energy sampling technology, they demonstrated the existence of a dynamic coordination structure formed by simultaneous interaction between cations and the two O atoms in *OCCO, which was found essential in promoting the formation C_2 products.

In addition to alkali metal cations, organic cations are also adopted in eCO_2R to regulate C_{2+} production. Different from alkali metal cations, organic cations generally exhibit a much larger hydration radius, the hydrophilicity of which can be tuned by adjusting their functional groups. And the catalytic activity and selectivity of eCO_2R can thereby be regulated in a broader range than alkaline metal cations due to the large variety of functional groups in organic cations. Moreover, other than electrostatic interactions, organic cations can also provide covalent and coordination interactions exhibiting specific nonelectric field effect. For instance, Li et al. determined via surface-enhanced infrared absorption spectroscopy and found that the variation in interfacial electric field strengths associated with the four different quaternary alkyl ammonium cations (alkyl$^4N^+$) remained negligible.[76] By analyzing the O–D stretching bands of interfacial heavy water (D_2O) on CO-covered Cu electrode, they attributed C_2H_4 formation to the presence of a water layer on the loading of different cations, whose hydrogen bonding stabilized *OCCO and enhanced eCO_2R. It is therefore evident that cations can serve as catalytic promoters in eCO_2R.

3.3. Anion Effect. In addition to cations, anions in the electrolyte can also improve the selectivity and activity of C_{2+} products by modulating the local pH. Hori et al. found that the local pH at the electrode–electrolyte interface becomes higher

https://doi.org/10.1021/acs.jpcc.4c00021
J. Phys. Chem. C XXXX, XXX, XXX–XXX

in nonbuffering KCl, $KClO_4$, and K_2SO_4 electrolytes, resulting in an increased selectivity for C_2H_4 on polycrystalline Cu.[54]

Other than modulating local pH, anions can also influence eCO_2R via their adsorption. For instance, Gao et al. mixed KCl, KBr, or KI (nonbuffered) in $KHCO_3$ (buffered) and obtained electrolytes exhibiting similar local pH values.[52] However, variations in the catalytic performance of preoxidized Cu surface in these electrolytes were observed. The current densities of C_2H_4 and CH_3CH_2OH production increased in response to changes in the anions ($Cl^- \rightarrow Br^- \rightarrow I^-$), confirming that factors other than pH contributed to the improvement in C_{2+} production, which was later hypothesized to be anion adsorption. Similarly, Shaw et al. found that the presence of adsorbed anions (F^- and Cl^-) can induce a decrease of almost 0.2 eV in *CO binding via DFT calculations,[77] which was further confirmed by Huang et al. According to the integrated charges of the CO adsorption peaks in linear sweep voltammetry, *CO coverage increased when the anion changed from $ClO_4^- \rightarrow Cl^- \rightarrow Br^- \rightarrow I^-$ (Figure 5a),[53] subsequently lowering the energetic barrier for *OCCO formation. In addition, the adsorbed anion can facilitate CO dimerization by modulating the electronic structure of local Cu sites, causing the carbon atoms on the *CO adsorbate on the adjacent adsorption sites to possess opposite charges, thereby creating electrostatic attraction. Apart from the electronic structure of active sites, anions can also promote the formation of C_{2+} products by influencing the electrode composition. For example, Qi et al. utilized a strong carbonate electrolyte to modulate the composition of the CuAg catalyst.[78] The carbonate anions were responsible for keeping the CO_2 concentration above the saturation limit and inhibiting the electrical displacement reaction that led to the separation of the Cu and Ag phases, realizing the formation of a stable CuAg alloy catalyst, which was found to exhibit enhanced formation rates of *CO and $*OCH_2CH_3$ and can produce C_3 chemicals. The above works revealed that the interaction between anions and catalysts can promote the generation of C_{2+} products through different mechanisms. However, the anion−catalyst interactions are not always beneficial for C_{2+} production, as the anions can poison the electrode surface under cathodic conditions especially when they do not directly participate in eCO_2R as carbonate and bicarbonate anions. As demonstrated by Bagger et al., the anion poisoning effect on eCO_2R can be quantified by describing the coverage of adsorbates as functions of potential.[79] As shown by AIMD[80,81] simulations of explicit electrolytes, the adsorption of *OCCOH, the trackable intermediate right after *OCCO, can be suppressed by anion adsorption (*OH, $*HPO_4$, $*PO_4$, $*CO_3$) at low overpotential, thereby limiting the onset potential of C_2H_4 generation (Figure 5b). The poisoning effect of anions is anticipated to induce a great influence on C_2 intermediates such as *OCCO and *OCCOH that have to occupy two adsorption sites, making them more prone to dissociation and desorption. Thus, the anion poisoning effect remains nonnegligible in the synthesis of C_{2+} products.

4. SUMMARY AND OUTLOOK

In summary, the generation of high-value multicarbon products from eCO_2R is a complex process that involves multiple reaction steps, intermediates, and pathways, yielding it highly sensitive to the electrolyte pH as well as the ions in solution. In particular, *OCCO formation is found to be the key intermediate in the conversion of CO_2 to multicarbon products, which exhibits dependence on both electrolyte pH and ions to some extent. By affecting the availability of H^+ and OH^- in the solution, pH is demonstrated to have a direct influence on pathways involving PCET. The difference in RLS can translate to variations in pH dependence of different products such as C_1 vs C_{2+} and C_2 oxygenates vs hydrocarbons, providing new possibilities to steer eCO_2R selectivity. Apart from the general effect to promote the production of C_{2+} chemicals via affecting PCET with water as the proton source, alkaline pH condition also promotes chemical reactions such as disproportionation reactions, offering new possibilities to synthesize acetate and higher-order multicarbon products. However, excessive pH can cause substantial CO_2 consumption and mitigate the overall catalytic performance of eCO_2R, and the inevitable reaction between CO_2 and OH^- may shift the local pH beyond the optimal region. Therefore, the high pH and CO_2 mass transport need to be delicately balanced in conventional one-pot CO_2 electrolysis to ensure an ideal C_{2+} production. Cations and anions in the electrolyte can also improve selectivity for C_{2+} products by adjusting the local pH. In addition, cations were mostly proposed to stabilize the reaction intermediates with substantial dipole moments through the generated electrical field, thereby enhancing C−C coupling, which can lead to the final multicarbon production. Such an effect was shown to be sensitive to a number of factors, such as the cation size, the geometric structure of electrodes, as well as the applied potential in electrolyte. Cations can also impact eCO_2R via the nonelectric field effect, as they were demonstrated to interact with surface adsorbates directly or indirectly. Similarly, anions were proposed to influence the adsorbate binding energy, leading to possible enhancement in the corresponding reaction energetics. The adsorption of anions, on the other hand, can poison the catalyst surface, necessitating a careful choice of the anion type and concentration.

Though research of the electrolyte effect has progressed considerably, there are still many challenges that deserve further attention from researchers, from both aspects of fundamental understanding and practical applications. Fundamentally, the effects of pH, cation, and anion are often entangled due to the ion complexation and the exchange of protons between ions and water. Disentangling their individual contribution to catalytic performance still requires more efforts with the assistance of advanced computations, in situ/operando characterizations, and delicately designed model experiments. While theoretical simulations are widely adopted to understand the electrolyte effects, we argue that an effective theoretical model of the electrified interface must adapt to the dynamic variations in local pH, ion distribution, and interfacial water structures. Recent advancement in characterizing and modeling alkaline HER has demonstrated the dependence of interfacial water structures, electric double layer properties, and reaction kinetics on pH, potential bias, and ion concentration.[82,83] We look forward to similar progress in eCO_2R. Apart from pH, the ion in the electrolyte presents another degree of difficulty in theoretical investigations. The presence of some anions (e.g., phosphate and bicarbonate ions) that buffer the interfacial pH can be used as proton donors, and how the shift of proton donor from water to them can affect PCET or PT barriers needs further exploration. Furthermore, more efforts are required to study the ion adsorption effects, where many current theoretical studies still lack the

https://doi.org/10.1021/acs.jpcc.4c00021
J. Phys. Chem. C XXXX, XXX, XXX−XXX

consideration of specific adsorption location of ions as well as the influence of ion adsorption on the deformation or reconstruction of catalytic surfaces. Moreover, beyond the above three components of electrolyte effects, the effects of other nonaqueous (co)solvents such as ionic liquids, if applicable, deserve further theoretical investigations since some experimental studies have unraveled distinct electrocatalytic behaviors in an aprotic environment.[84,85] Finally, we would like to emphasize that given the extreme complexity of interfacial electrolyte chemistry and the large variety of reaction pathways for eCO_2R, the full explicit modeling presents a grand challenge of theoretical electrocatalysis. A less computationally intensive approach to navigate through the vast chemical complexities therefore remains vital.

In addition to fundamental understanding, better leveraging of the beneficial electrolyte effects in practical applications of eCO_2R also asks for continuous future efforts. High pH in general promotes C_{2+} production, but the reaction between OH^- and CO_2 becomes more pronounced simultaneously, leading to carbonate formation and irreversible acidification of the electrolyte. The resulting carbonates can block the reactor channels while the acidified electrolyte can induce a switch of product selectivity from C_{2+} to C_1 and hydrogen. As we pointed out before, the tandem reactor design that decouples the whole process into two individual units for eCO_2R to CO and eCOR to C_{2+} provides a feasible way of separate process optimization, mitigating the detrimental carbonation at high pH. However, an issue that cannot be circumvented by the tandem reactor engineering is the adoption of anion exchange membrane for alkaline electrolysis. So far, the ionic conductivity and durability of the anion exchange membrane are still incomparable to those of proton exchange membranes, limiting the catalytic performance of the second alkaline electrolysis unit in a tandem system. The improvement of membrane materials is thereby necessary. Additionally, the corrosion or aging effect on catalysts and other cell components under highly alkaline conditions remains non-negligible, making it imperative to investigate and improve the stability of eCO_2R catalysts (e.g., Cu) under practical conditions (e.g., high current density, higher temperature, and larger potential bias). Implementing the benefits of ion effects in practical CO_2 electrolysis, such as the local reaction microenvironment modulation to obtain more C_{2+} products, also has potential risks of increasing the separation cost and cell voltage, due to salt precipitation and possibly decreased electrolyte conductivity. The combination of solid-electrolyte-based reactors and ion-immobilization strategies could be a promising solution to simultaneously inhibit salt contamination and modulate reaction microenvironments. Nevertheless, similar to the challenges for fundamental understanding, the impacts on eCO_2R introduced by electrolytes are usually convoluted, making it extremely hard to disentangle and isolate various effects experimentally, which also places implicit obstacles on the systematic optimization and rational design of electrolytes. We thus encourage future research to consider the catalyst, the electrolyte, and the reactor in a comprehensive codesign scheme.

With the rapid development of artificial intelligence, machine learning (ML)-based techniques start to bring in new opportunities to ease the computational burden of reaction exploration and system optimization in other sectors of chemical research such as secondary batteries,[86−88] as they can help to simplify the detailed modeling of complex reaction mechanisms as well as to learn important patterns from vast experimental and computational data. The boosted computing power can also potentially allow for more realistic simulations of the electrical interfaces. More importantly, a tight linking of experiments, theory, and machine learning can greatly facilitate data reproducibility and reusability. Overall, we believe that such a multidisciplinary research approach can greatly improve our understanding of the field and promote research efficiency while conserving resources. eCO_2R, as a promising technology lighting the sustainable future, will definitely benefit from that.

AUTHOR INFORMATION

Corresponding Authors

Chuan Xia − *School of Materials and Energy, University of Electronic Science and Technology of China, Chengdu, Sichuan 611731, P. R. China;* orcid.org/0000-0003-4526-159X; Email: chuan.xia@uestc.edu.cn

Xinyan Liu − *Institute of Fundamental and Frontier Sciences and Key Laboratory of Quantum Physics and Photonic Quantum Information, Ministry of Education, University of Electronic Science and Technology of China, Chengdu, Sichuan 611731, P. R. China;* orcid.org/0000-0002-3629-1730; Email: xinyanl@uestc.edu.cn

Authors

Xian Zhong − *School of Materials and Energy, University of Electronic Science and Technology of China, Chengdu, Sichuan 611731, P. R. China; Institute of Fundamental and Frontier Sciences, University of Electronic Science and Technology of China, Chengdu, Sichuan 611731, P. R. China*

Hong-Jie Peng − *Institute of Fundamental and Frontier Sciences, University of Electronic Science and Technology of China, Chengdu, Sichuan 611731, P. R. China;* orcid.org/0000-0002-4183-703X

Complete contact information is available at: https://pubs.acs.org/10.1021/acs.jpcc.4c00021

Notes

The authors declare no competing financial interest.

Biographies

Xian Zhong graduated from Chang'an University with a bachelor degree in 2021. Now she is pursuing a master degree under the joint supervision of Dr. Xinyan Liu and Prof. Chuan Xia at University of Electronic Science and Technology of China (UESTC). Her research interests mainly focus on first-principle calculations for applications such as electrocatalytic CO_2 reduction, water splitting, and high-energy secondary batteries.

Hong-Jie Peng is a Professor at Institute of Fundamental and Frontier Sciences (IFFS), University of Electronic Science and Technology of China (UESTC). He obtained B.S. and Ph.D. degrees at Department of Chemical Engineering, Tsinghua University, in 2013 and 2018, respectively. He was a postdoctoral fellow at SUNCAT center, Stanford University, during 2018−2020. He was selected as Highly Cited Researchers at 2019−2023 by Clarivate Analytics. His current research interests are advanced energy chemistry and energy materials, including high-energy rechargeable batteries, renewable electrocatalysis, theoretical tools, and data-driven methods.

Chuan Xia is a Professor of Materials and Energy at University of Electronic Science and Technology of China (UESTC). He obtained his Bachelor from Beijing University of Technology in 2012 and his Ph.D. at King Abdullah University of Science and Technology in 2018, followed by a postdoctoral Fellowship at Harvard University

https://doi.org/10.1021/acs.jpcc.4c00021
J. Phys. Chem. C XXXX, XXX, XXX−XXX

and Rice University. In 2020 he joined UESTC, where he initiated an active research group focusing on developing methods for controlling the architecture of molecules and materials, understanding their fundamental properties, and utilizing such structures to develop novel catalysts that can be applied in the areas of electrocatalysis, energy generation, storage, and conversion. More information about Dr. Xia and his research can be found here: www.chuan-lab.com

Xinyan Liu is a Research Professor at Institute of Fundamental and Frontier Sciences (IFFS), University of Electronic Science and Technology of China (UESTC). Having obtained her bachelor and Ph.D. degree from Tsinghua University and Stanford University in 2013 and 2018, respectively, she worked at Meta Inc. for two years as a Research Data Scientist before she joined full time at UESTC. Dr. Liu's research interest has been mainly focused on the energy chemistry-related interdisciplinary study combining theoretical simulations and artificial intelligence, such as electrocatalysis, catalyst high-throughput screening, and battery prognosis.

■ ACKNOWLEDGMENTS

This work was supported by National Natural Science Foundation of China (22109020, 22109082, and 22379021) and Sichuan Science and Technology Program (2023NSFSC0115). C.X. acknowledges the National Key Research and Development Program of China (2022YFB4102000), National Natural Science Foundation of China (22102018 and 52171201), the Huzhou Science and Technology Bureau (2022GZ45).

■ REFERENCES

(1) Kong, X.; Wang, C.; Zheng, H.; Geng, Z.; Bao, J.; Zeng, J. Enhance the Activity of Multi-Carbon Products for Cu via P Doping towards CO_2 Reduction. *Sci. China Chem.* **2021**, *64*, 1096−1102.
(2) Ng, S.-F.; Foo, J. J.; Ong, W.-J. Solar-Powered Chemistry: Engineering Low-Dimensional Carbon Nitride-Based Nanostructures for Selective CO_2 Conversion to C_1-C_2 Products. *InfoMat* **2022**, *4*, No. e12279.
(3) Luo, Y.; Zhang, K.; Li, Y.; Wang, Y. Valorizing Carbon Dioxide via Electrochemical Reduction on Gas-Diffusion Electrodes. *InfoMat* **2021**, *3*, 1313−1332.
(4) Verdaguer-Casadevall, A.; Li, C. W.; Johansson, T. P.; Scott, S. B.; McKeown, J. T.; Kumar, M.; Stephens, I. E. L.; Kanan, M. W.; Chorkendorff, I. Probing the Active Surface Sites for CO Reduction on Oxide-Derived Copper Electrocatalysts. *J. Am. Chem. Soc.* **2015**, *137*, 9808−9811.
(5) Gu, J.; Hsu, C.-S.; Bai, L.; Chen, H. M.; Hu, X. Atomically Dispersed Fe^{3+} Sites Catalyze Efficient CO_2 Electroreduction to CO. *Science* **2019**, *364*, 1091−1094.
(6) Shi, R.; Guo, J.; Zhang, X.; Waterhouse, G. I. N.; Han, Z.; Zhao, Y.; Shang, L.; Zhou, C.; Jiang, L.; Zhang, T. Efficient Wettability-Controlled Electroreduction of CO_2 to CO at Au/C Interfaces. *Nat. Commun.* **2020**, *11*, 3028.
(7) Li, Q.-X.; Si, D.-H.; Lin, W.; Wang, Y.-B.; Zhu, H.-J.; Huang, Y.-B.; Cao, R. Highly Efficient Electroreduction of CO_2 by Defect Single-Atomic Ni-N_3 Sites Anchored on Ordered Micro-Macroporous Carbons. *Sci. China Chem.* **2022**, *65*, 1584−1593.
(8) Ren, X.; Liu, S.; Li, H.; Ding, J.; Liu, L.; Kuang, Z.; Li, L.; Yang, H.; Bai, F.; Huang, Y.; et al. Electron-Withdrawing Functional Ligand Promotes CO_2 Reduction Catalysis in Single Atom Catalyst. *Sci. China Chem.* **2020**, *63*, 1727−1733.
(9) Zheng, T.; Liu, C.; Guo, C.; Zhang, M.; Li, X.; Jiang, Q.; Xue, W.; Li, H.; Li, A.; Pao, C.-W.; et al. Copper-Catalysed Exclusive CO_2 to Pure Formic Acid Conversion via Single-Atom Alloying. *Nat. Nanotechnol.* **2021**, *16*, 1386−1393.
(10) Li, Z.; Cao, A.; Zheng, Q.; Fu, Y.; Wang, T.; Arul, K. T.; Chen, J.-L.; Yang, B.; Adli, N. M.; Lei, L.; et al. Elucidation of the Synergistic Effect of Dopants and Vacancies on Promoted Selectivity for CO_2 Electroreduction to Formate. *Adv. Mater.* **2021**, *33*, 2005113.
(11) Gao, T.; Kumar, A.; Shang, Z.; Duan, X.; Wang, H.; Wang, S.; Ji, S.; Yan, D.; Luo, L.; Liu, W.; et al. Promoting Electrochemical Conversion of CO_2 to Formate with Rich Oxygen Vacancies in Nanoporous Tin Oxides. *Chin. Chem. Lett.* **2019**, *30*, 2274−2278.
(12) Sun, H.; Liu, J. Carbon-Supported CoS_4-C Single-Atom Nanozyme for Dramatic Improvement in CO_2 Electroreduction to HCOOH: A DFT Study Combined with Hybrid Solvation Model. *Chin. Chem. Lett.* **2023**, *34*, 108018.
(13) Zhang, Y.; Chen, Y.; Liu, R.; Wang, X.; Liu, H.; Zhu, Y.; Qian, Q.; Feng, Y.; Cheng, M.; Zhang, G. Oxygen Vacancy Stabilized $Bi_2O_2CO_3$ Nanosheet for CO_2 Electroreduction at Low Overpotential Enables Energy Efficient CO-Production of Formate. *InfoMat* **2023**, *5*, No. e12375.
(14) Dai, Y.; Li, H.; Wang, C.; Xue, W.; Zhang, M.; Zhao, D.; Xue, J.; Li, J.; Luo, L.; Liu, C.; et al. Manipulating Local Coordination of Copper Single Atom Catalyst Enables Efficient CO_2-to-CH_4 Conversion. *Nat. Commun.* **2023**, *14*, 3382.
(15) Zhang, Y.; Dong, L.-Z.; Li, S.; Huang, X.; Chang, J.-N.; Wang, J.-H.; Zhou, J.; Li, S.-L.; Lan, Y.-Q. Coordination Environment Dependent Selectivity of Single-Site-Cu Enriched Crystalline Porous Catalysts in CO_2 Reduction to CH_4. *Nat. Commun.* **2021**, *12*, 6390.
(16) Liu, X.; Xiao, J.; Peng, H.; Hong, X.; Chan, K.; Nørskov, J. K. Understanding Trends in Electrochemical Carbon Dioxide Reduction Rates. *Nat. Commun.* **2017**, *8*, 15438.
(17) Wu, Y.; Jiang, Z.; Lu, X.; Liang, Y.; Wang, H. Domino Electroreduction of CO_2 to Methanol on a Molecular Catalyst. *Nature* **2019**, *575*, 639−642.
(18) Lu, L.; Sun, X.; Ma, J.; Yang, D.; Wu, H.; Zhang, B.; Zhang, J.; Han, B. Highly Efficient Electroreduction of CO_2 to Methanol on Palladium-Copper Bimetallic Aerogels. *Angew. Chem., Int. Ed.* **2018**, *57*, 14149−14153.
(19) Liu, X.; Li, B.-Q.; Ni, B.; Wang, L.; Peng, H.-J. A Perspective on the Electrocatalytic Conversion of Carbon Dioxide to Methanol with Metallomacrocyclic Catalysts. *J. Energy Chem.* **2022**, *64*, 263−275.
(20) Bushuyev, O. S.; De Luna, P.; Dinh, C. T.; Tao, L.; Saur, G.; van de Lagemaat, J.; Kelley, S. O.; Sargent, E. H. What Should We Make with CO_2 and How Can We Make It? *Joule* **2018**, *2*, 825−832.
(21) Peng, H.-J.; Tang, M. T.; Halldin Stenlid, J.; Liu, X.; Abild-Pedersen, F. Trends in Oxygenate/Hydrocarbon Selectivity for Electrochemical $CO_{(2)}$ Reduction to C_2 Products. *Nat. Commun.* **2022**, *13*, 1399.
(22) Peng, H.; Tang, M. T.; Liu, X.; Lamoureux, P. S.; Bajdich, M.; Abild-Pedersen, F. The Role of Atomic Carbon in Directing Electrochemical $CO_{(2)}$ Reduction to Multicarbon Products. *Energy Environ. Sci.* **2021**, *14*, 473−482.
(23) Gao, D.; Arán-Ais, R. M.; Jeon, H. S.; Roldan Cuenya, B. Rational Catalyst and Electrolyte Design for CO_2 Electroreduction towards Multicarbon Products. *Nat. Catal.* **2019**, *2*, 198−210.
(24) Calvinho, K. U. D.; Laursen, A. B.; Yap, K. M. K.; Goetjen, T. A.; Hwang, S.; Murali, N.; Mejia-Sosa, B.; Lubarski, A.; Teeluck, K. M.; Hall, E. S.; et al. Selective CO_2 Reduction to C_3 and C_4 Oxyhydrocarbons on Nickel Phosphides at Overpotentials as Low as 10 mV. *Energy Environ. Sci.* **2018**, *11*, 2550−2559.
(25) Gao, Z.; Li, J.; Zhang, Z.; Hu, W. Recent Advances in Carbon-Based Materials for Electrochemical CO_2 Reduction Reaction. *Chin. Chem. Lett.* **2022**, *33*, 2270−2280.
(26) Qin, T.; Qian, Y.; Zhang, F.; Lin, B.-L. Cloride-Derived Copper Electrode for Efficient Electrochemical Reduction of CO_2 to Ethylene. *Chin. Chem. Lett.* **2019**, *30*, 314−318.
(27) Xue, W.; Liu, H.; Chen, X.; Yang, X.; Yang, R.; Liu, Y.; Li, M.; Yang, X.; Xia, B. Y.; You, B. Operando Reconstruction towards Stable CuI Nanodots with Favorable Facets for Selective CO_2 Electroreduction to C_2H_4. *Sci. China Chem.* **2023**, *66*, 1834−1843.
(28) Wang, L.; Nitopi, S. A.; Bertheussen, E.; Orazov, M.; Morales-Guio, C. G.; Liu, X.; Higgins, D. C.; Chan, K.; Nørskov, J. K.; Hahn, C.; et al. Electrochemical Carbon Monoxide Reduction on Polycrystalline Copper: Effects of Potential, Pressure, and pH on

https://doi.org/10.1021/acs.jpcc.4c00021
J. Phys. Chem. C XXXX, XXX, XXX−XXX

Selectivity toward Multicarbon and Oxygenated Products. *ACS Catal.* **2018**, *8*, 7445−7454.
(29) Sebastián-Pascual, P.; Petersen, A. S.; Bagger, A.; Rossmeisl, J.; Escudero-Escribano, M. pH and Anion Effects on Cu-Phosphate Interfaces for CO Electroreduction. *ACS Catal.* **2021**, *11*, 1128−1135.
(30) Resasco, J.; Chen, L. D.; Clark, E.; Tsai, C.; Hahn, C.; Jaramillo, T. F.; Chan, K.; Bell, A. T. Promoter Effects of Alkali Metal Cations on the Electrochemical Reduction of Carbon Dioxide. *J. Am. Chem. Soc.* **2017**, *139*, 11277−11287.
(31) Schouten, K. J. P.; Kwon, Y.; van der Ham, C. J. M.; Qin, Z.; Koper, M. T. M. A New Mechanism for the Selectivity to C_1 and C_2 Species in the Electrochemical Reduction of Carbon Dioxide on Copper Electrodes. *Chem. Sci.* **2011**, *2*, 1902−1909.
(32) Zhan, C.; Dattila, F.; Rettenmaier, C.; Bergmann, A.; Kühl, S.; García-Muelas, R.; López, N.; Cuenya, B. R. Revealing the CO Coverage-Driven C-C Coupling Mechanism for Electrochemical CO_2 Reduction on Cu_2O Nanocubes via Operando Raman Spectroscopy. *ACS Catal.* **2021**, *11*, 7694−7701.
(33) An, H.; Wu, L.; Mandemaker, L. D. B.; Yang, S.; de Ruiter, J.; Wijten, J. H. J.; Janssens, J. C. L.; Hartman, T.; van der Stam, W.; Weckhuysen, B. M. Sub-Second Time-Resolved Surface-Enhanced Raman Spectroscopy Reveals Dynamic CO Intermediates during Electrochemical CO_2 Reduction on Copper. *Angew. Chem., Int. Ed.* **2021**, *60*, 16576−16584.
(34) Pérez-Gallent, E.; Figueiredo, M. C.; Calle-Vallejo, F.; Koper, M. T. M. Spectroscopic Observation of a Hydrogenated CO Dimer Intermediate During CO Reduction on Cu(100) Electrodes. *Angew. Chem., Int. Ed.* **2017**, *56*, 3621−3624.
(35) Calle-Vallejo, F.; Koper, M. T. M. Theoretical Considerations on the Electroreduction of CO to C_2 Species on Cu(100) Electrodes. *Angew. Chem., Int. Ed.* **2013**, *52*, 7282−7285.
(36) Montoya, J. H.; Shi, C.; Chan, K.; Nørskov, J. K. Theoretical Insights into a CO Dimerization Mechanism in CO_2 Electroreduction. *J. Phys. Chem. Lett.* **2015**, *6*, 2032−2037.
(37) Hedström, S.; dos Santos, E. C.; Liu, C.; Chan, K.; Abild-Pedersen, F.; Pettersson, L. G. M. Spin Uncoupling in Chemisorbed OCCO and CO_2: Two High-Energy Intermediates in Catalytic CO_2 Reduction. *J. Phys. Chem. C* **2018**, *122*, 12251−12258.
(38) Nitopi, S.; Bertheussen, E.; Scott, S. B.; Liu, X.; Engstfeld, A. K.; Horch, S.; Seger, B.; Stephens, I. E. L.; Chan, K.; Hahn, C.; et al. Progress and Perspectives of Electrochemical CO_2 Reduction on Copper in Aqueous Electrolyte. *Chem. Rev.* **2019**, *119*, 7610−7672.
(39) Chang, B.; Pang, H.; Raziq, F.; Wang, S.; Huang, K.-W.; Ye, J.; Zhang, H. Electrochemical Reduction of Carbon Dioxide to Multicarbon (C_{2+}) Products: Challenges and Perspectives. *Energy Environ. Sci.* **2023**, *16*, 4714−4758.
(40) Dattila, F.; Seemakurthi, R. R.; Zhou, Y.; López, N. Modeling Operando Electrochemical CO_2 Reduction. *Chem. Rev.* **2022**, *122*, 11085−11130.
(41) Hori, Y.; Takahashi, R.; Yoshinami, Y.; Murata, A. Electrochemical Reduction of CO at a Copper Electrode. *J. Phys. Chem. B* **1997**, *101*, 7075−7081.
(42) Iyengar, P.; Kolb, M. J.; Pankhurst, J. R.; Calle-Vallejo, F.; Buonsanti, R. Elucidating the Facet-Dependent Selectivity for CO_2 Electroreduction to Ethanol of Cu-Ag Tandem Catalysts. *ACS Catal.* **2021**, *11*, 4456−4463.
(43) Garza, A. J.; Bell, A. T.; Head-Gordon, M. Mechanism of CO_2 Reduction at Copper Surfaces: Pathways to C_2 Products. *ACS Catal.* **2018**, *8*, 1490−1499.
(44) Santatiwongchai, J.; Faungnawakij, K.; Hirunsit, P. Comprehensive Mechanism of CO_2 Electroreduction toward Ethylene and Ethanol: The Solvent Effect from Explicit Water-Cu(100) Interface Models. *ACS Catal.* **2021**, *11*, 9688−9701.
(45) Goodpaster, J. D.; Bell, A. T.; Head-Gordon, M. Identification of Possible Pathways for C-C Bond Formation during Electrochemical Reduction of CO_2: New Theoretical Insights from an Improved Electrochemical Model. *J. Phys. Chem. Lett.* **2016**, *7*, 1471−1477.
(46) Liu, Q.; Zhang, X.-G.; Du, Z.-Y.; Zou, C.-J.; Chen, H.-Y.; Zhao, Y.; Dong, J.-C.; Fang, P.-P.; Li, J.-F. Converting CO_2 to Ethanol on Ag Nanowires with High Selectivity Investigated by Operando Raman Spectroscopy. *Sci. China Chem.* **2023**, *66*, 259−265.
(47) Li, Q.; Zhang, Y.; Shi, L.; Wu, M.; Ouyang, Y.; Wang, J. Dynamic Structure Change of Cu Nanoparticles on Carbon Supports for CO_2 Electro-Reduction toward Multicarbon Products. *InfoMat* **2021**, *3*, 1285−1294.
(48) Xiao, H.; Cheng, T.; Goddard, W. A. I. Atomistic Mechanisms Underlying Selectivities in C_1 and C_2 Products from Electrochemical Reduction of CO on Cu(111). *J. Am. Chem. Soc.* **2017**, *139*, 130−136.
(49) da Silva, A. H. M.; Lenne, Q.; Vos, R. E.; Koper, M. T. M. Competition of CO and Acetaldehyde Adsorption and Reduction on Copper Electrodes and Its Impact on N-Propanol Formation. *ACS Catal.* **2023**, *13*, 4339−4347.
(50) Dong, Y.; Ma, M.; Jiao, Z.; Han, S.; Xiong, L.; Deng, Z.; Peng, Y. Effect of Electrolyte Cation-Mediated Mechanism on Electrocatalytic Carbon Dioxide Reduction. *Chin. Chem. Lett.* **2023**, 109049.
(51) Ringe, S.; Clark, E. L.; Resasco, J.; Walton, A.; Seger, B.; Bell, A. T.; Chan, K. Understanding Cation Effects in Electrochemical CO_2 Reduction. *Energy Environ. Sci.* **2019**, *12*, 3001−3014.
(52) Gao, D.; Scholten, F.; Roldan Cuenya, B. Improved CO_2 Electroreduction Performance on Plasma-Activated Cu Catalysts via Electrolyte Design: Halide Effect. *ACS Catal.* **2017**, *7*, 5112−5120.
(53) Huang, Y.; Ong, C. W.; Yeo, B. S. Effects of Electrolyte Anions on the Reduction of Carbon Dioxide to Ethylene and Ethanol on Copper (100) and (111) Surfaces. *ChemSusChem* **2018**, *11*, 3299−3306.
(54) Hori, Y.; Murata, A.; Takahashi, R.; Suzuki, S. Electroreduction of Carbon Monoxide to Methane and Ethylene at a Copper Electrode in Aqueous Solutions at Ambient Temperature and Pressure. *J. Am. Chem. Soc.* **1987**, *109*, 5022−5023.
(55) Hori, Y.; Murata, A.; Takahashi, R. Formation of Hydrocarbons in the Electrochemical Reduction of Carbon Dioxide at a Copper Electrode in Aqueous Solution. *J. Chem. Soc., Faraday Trans. 1* **1989**, *85*, 2309−2326.
(56) Nørskov, J. K.; Studt, F.; Abild-Pedersen, F.; Bligaard, T. *Fundamental concepts in heterogeneous catalysis*; John Wiley & Sons, Ltd., 2014.
(57) Liu, X.; Schlexer, P.; Xiao, J.; Ji, Y.; Wang, L.; Sandberg, R. B.; Tang, M.; Brown, K. S.; Peng, H.; Ringe, S.; et al. pH Effects on the Electrochemical Reduction of $CO_{(2)}$ towards C_2 Products on Stepped Copper. *Nat. Commun.* **2019**, *10*, 32.
(58) Xiao, H.; Cheng, T.; Goddard, W. A. I.; Sundararaman, R. Mechanistic Explanation of the pH Dependence and Onset Potentials for Hydrocarbon Products from Electrochemical Reduction of CO on Cu (111). *J. Am. Chem. Soc.* **2016**, *138*, 483−486.
(59) Birdja, Y. Y.; Koper, M. T. M. The Importance of Cannizzaro-Type Reactions during Electrocatalytic Reduction of Carbon Dioxide. *J. Am. Chem. Soc.* **2017**, *139*, 2030−2034.
(60) Jouny, M.; Luc, W.; Jiao, F. High-Rate Electroreduction of Carbon Monoxide to Multi-Carbon Products. *Nat. Catal.* **2018**, *1*, 748−755.
(61) Jouny, M.; Lv, J.-J.; Cheng, T.; Ko, B. H.; Zhu, J.-J.; Goddard, W. A.; Jiao, F. Formation of Carbon-Nitrogen Bonds in Carbon Monoxide Electrolysis. *Nat. Chem.* **2019**, *11*, 846−851.
(62) Heenen, H. H.; Shin, H.; Kastlunger, G.; Overa, S.; Gauthier, J. A.; Jiao, F.; Chan, K. The Mechanism for Acetate Formation in Electrochemical $CO_{(2)}$ Reduction on Cu: Selectivity with Potential, pH, and Nanostructuring. *Energy Environ. Sci.* **2022**, *15*, 3978−3990.
(63) Ting, L. R. L.; García-Muelas, R.; Martín, A. J.; Veenstra, F. L. P.; Chen, S. T.-J.; Peng, Y.; Per, E. Y. X.; Pablo-García, S.; López, N.; Pérez-Ramírez, J.; et al. Electrochemical Reduction of Carbon Dioxide to 1-Butanol on Oxide-Derived Copper. *Angew. Chem., Int. Ed.* **2020**, *59*, 21072−21079.
(64) Raciti, D.; Mao, M.; Wang, C. Mass Transport Modelling for the Electroreduction of CO_2 on Cu Nanowires. *Nanotechnology* **2018**, *29*, 044001.
(65) Lum, Y.; Yue, B.; Lobaccaro, P.; Bell, A. T.; Ager, J. W. Optimizing C-C Coupling on Oxide-Derived Copper Catalysts for

https://doi.org/10.1021/acs.jpcc.4c00021
J. Phys. Chem. C XXXX, XXX, XXX−XXX

Electrochemical CO_2 Reduction. *J. Phys. Chem. C* **2017**, *121*, 14191−14203.
(66) Jouny, M.; Hutchings, G. S.; Jiao, F. Carbon Monoxide Electroreduction as an Emerging Platform for Carbon Utilization. *Nat. Catal.* **2019**, *2*, 1062−1070.
(67) Murata, A.; Hori, Y. Product Selectivity Affected by Cationic Species in Electrochemical Reduction of CO_2 and CO at a Cu Electrode. *Bull. Chem. Soc. Jpn.* **1991**, *64*, 123−127.
(68) Frumkin, A. N. Influence of Cation Adsorption on the Kinetics of Electrode Processes. *Trans. Faraday Soc.* **1959**, *55*, 156−167.
(69) Singh, M. R.; Kwon, Y.; Lum, Y.; Ager, J. W. I.; Bell, A. T. Hydrolysis of Electrolyte Cations Enhances the Electrochemical Reduction of CO_2 over Ag and Cu. *J. Am. Chem. Soc.* **2016**, *138*, 13006−13012.
(70) Gunathunge, C. M.; Ovalle, V. J.; Waegele, M. M. Probing Promoting Effects of Alkali Cations on the Reduction of CO at the Aqueous Electrolyte/Copper Interface. *Phys. Chem. Chem. Phys.* **2017**, *19*, 30166−30172.
(71) Pérez-Gallent, E.; Marcandalli, G.; Figueiredo, M. C.; Calle-Vallejo, F.; Koper, M. T. M. Structure- and Potential-Dependent Cation Effects on CO Reduction at Copper Single-Crystal Electrodes. *J. Am. Chem. Soc.* **2017**, *139*, 16412−16419.
(72) Ren, W.; Xu, A.; Chan, K.; Hu, X. A Cation Concentration Gradient Approach to Tune the Selectivity and Activity of CO_2 Electroreduction. *Angew. Chem., Int. Ed.* **2022**, *61*, No. e202214173.
(73) Ludwig, T.; Gauthier, J. A.; Dickens, C. F.; Brown, K. S.; Ringe, S.; Chan, K.; Nørskov, J. K. Atomistic Insight into Cation Effects on Binding Energies in Cu-Catalyzed Carbon Dioxide Reduction. *J. Phys. Chem. C* **2020**, *124*, 24765−24775.
(74) Malkani, A. S.; Li, J.; Oliveira, N. J.; He, M.; Chang, X.; Xu, B.; Lu, Q. Understanding the electric and nonelectric field components of the cation effect on the electrochemical CO reduction reaction. *Sci. Adv.* **2020**, *6*, eabd2569.
(75) Liu, H.; Liu, J.; Yang, B. Promotional Role of a Cation Intermediate Complex in C_2 Formation from Electrochemical Reduction of CO_2 over Cu. *ACS Catal.* **2021**, *11*, 12336−12343.
(76) Li, J.; Li, X.; Gunathunge, C. M.; Waegele, M. M. Hydrogen Bonding Steers the Product Selectivity of Electrocatalytic CO Reduction. *Proc. Natl. Acad. Sci. U.S.A.* **2019**, *116*, 9220−9229.
(77) Shaw, S. K.; Berná, A.; Feliu, J. M.; Nichols, R. J.; Jacob, T.; Schiffrin, D. J. Role of Axially Coordinated Surface Sites for Electrochemically Controlled Carbon Monoxide Adsorption on Single Crystal Copper Electrodes. *Phys. Chem. Chem. Phys.* **2011**, *13*, 5242−5251.
(78) Qi, K.; Zhang, Y.; Onofrio, N.; Petit, E.; Cui, X.; Ma, J.; Fan, J.; Wu, H.; Wang, W.; Li, J.; et al. Unlocking Direct CO_2 Electrolysis to C_3 Products via Electrolyte Supersaturation. *Nat. Catal.* **2023**, *6*, 319−331.
(79) Bagger, A.; Arnarson, L.; Hansen, M. H.; Spohr, E.; Rossmeisl, J. Electrochemical CO Reduction: A Property of the Electrochemical Interface. *J. Am. Chem. Soc.* **2019**, *141*, 1506−1514.
(80) Naderian, M.; Groß, A. From Single Molecules to Water Networks: Dynamics of Water Adsorption on Pt(111). *J. Chem. Phys.* **2016**, *145*, 094703.
(81) Herron, J. A.; Morikawa, Y.; Mavrikakis, M. Ab Initio Molecular Dynamics of Solvation Effects on Reactivity at Electrified Interfaces. *Proc. Natl. Acad. Sci. U.S.A.* **2016**, *113*, No. E4937-E4945.
(82) Wang, Y.-H.; Zheng, S.; Yang, W.-M.; Zhou, R.-Y.; He, Q.-F.; Radjenovic, P.; Dong, J.-C.; Li, S.; Zheng, J.; Yang, Z.-L.; et al. In Situ Raman Spectroscopy Reveals the Structure and Dissociation of Interfacial Water. *Nature* **2021**, *600*, 81−85.
(83) Li, P.; Jiang, Y.; Hu, Y.; Men, Y.; Liu, Y.; Cai, W.; Chen, S. Hydrogen Bond Network Connectivity in the Electric Double Layer Dominates the Kinetic pH Effect in Hydrogen Electrocatalysis on Pt. *Nat. Catal.* **2022**, *5*, 900−911.
(84) Schreier, M.; Yoon, Y.; Jackson, M. N.; Surendranath, Y. Competition between H and CO for Active Sites Governs Copper-Mediated Electrosynthesis of Hydrocarbon Fuels. *Angew. Chem., Int. Ed.* **2018**, *57*, 10221−10225.
(85) Chu, A. T.; Surendranath, Y. Aprotic Solvent Exposes an Altered Mechanism for Copper-Catalyzed Ethylene Electrosynthesis. *J. Am. Chem. Soc.* **2022**, *144*, 5359−5365.
(86) Liu, X.; Cai, C.; Zhao, W.; Peng, H.-J.; Wang, T. Machine Learning-Assisted Screening of Stepped Alloy Surfaces for C_1 Catalysis. *ACS Catal.* **2022**, *12*, 4252−4260.
(87) Liu, X.; Peng, H.-J.; Li, B.-Q.; Chen, X.; Li, Z.; Huang, J.-Q.; Zhang, Q. Untangling Degradation Chemistries of Lithium-Sulfur Batteries Through Interpretable Hybrid Machine Learning. *Angew. Chem., Int. Ed.* **2022**, *134*, No. e202214037.
(88) Chen, A.; Zhang, X.; Zhou, Z. Machine Learning: Accelerating Materials Development for Energy Storage and Conversion. *InfoMat* **2020**, *2*, 553−576.

https://doi.org/10.1021/acs.jpcc.4c00021
J. Phys. Chem. C XXXX, XXX, XXX−XXX